



Universiteit
Leiden
The Netherlands

High-resolution karyotyping by oligonucleotide microarrays : the next revolution in cytogenetics

Gijsbers, A.C.J.

Citation

Gijsbers, A. C. J. (2010, November 30). *High-resolution karyotyping by oligonucleotide microarrays : the next revolution in cytogenetics*. Retrieved from <https://hdl.handle.net/1887/16187>

Version: Corrected Publisher's Version

License: [Licence agreement concerning inclusion of doctoral thesis in the Institutional Repository of the University of Leiden](#)

Downloaded from: <https://hdl.handle.net/1887/16187>

Note: To cite this publication please use the final published version (if applicable).

Appendix (color figures)

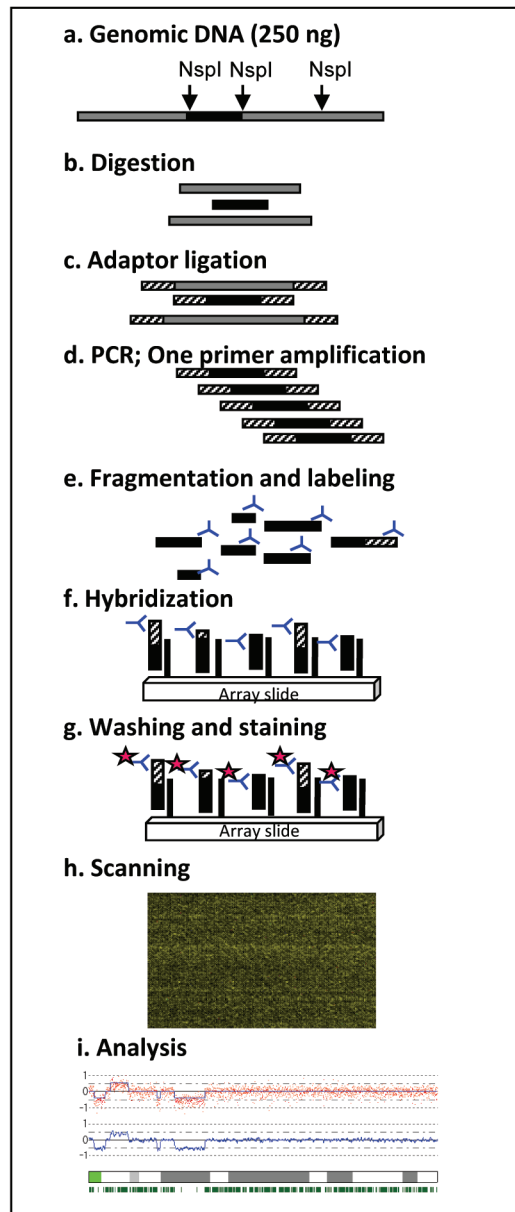


Figure 1.1 Schematic overview of the Affymetrix platform procedure

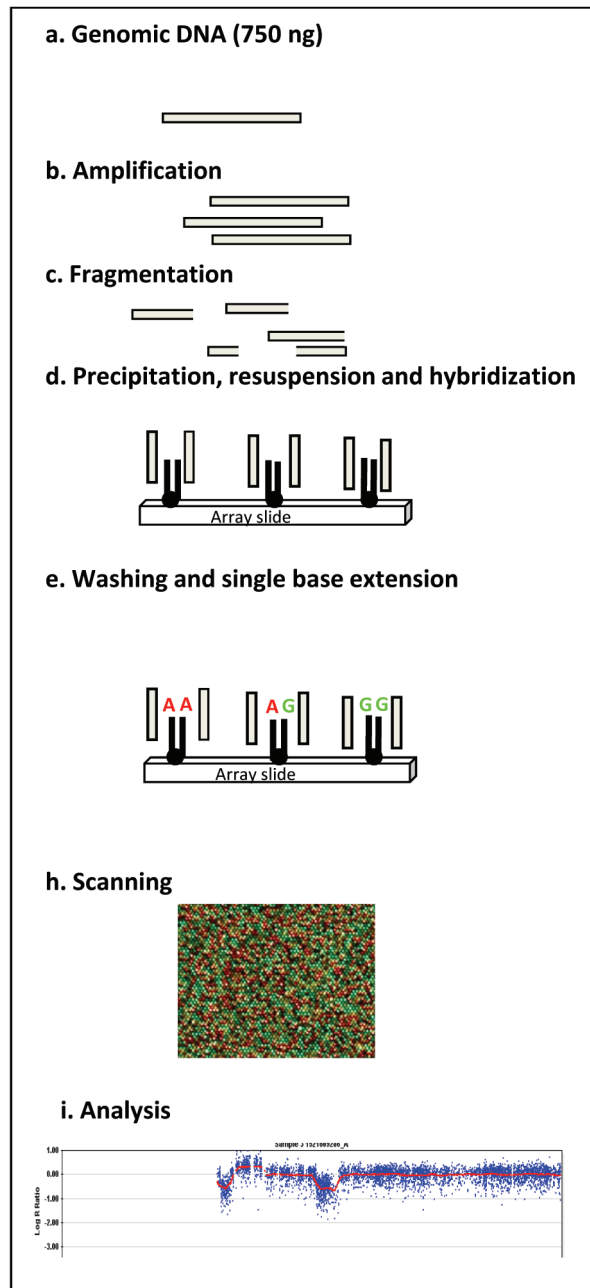


Figure 1.2 Schematic overview of the Illumina platform procedure

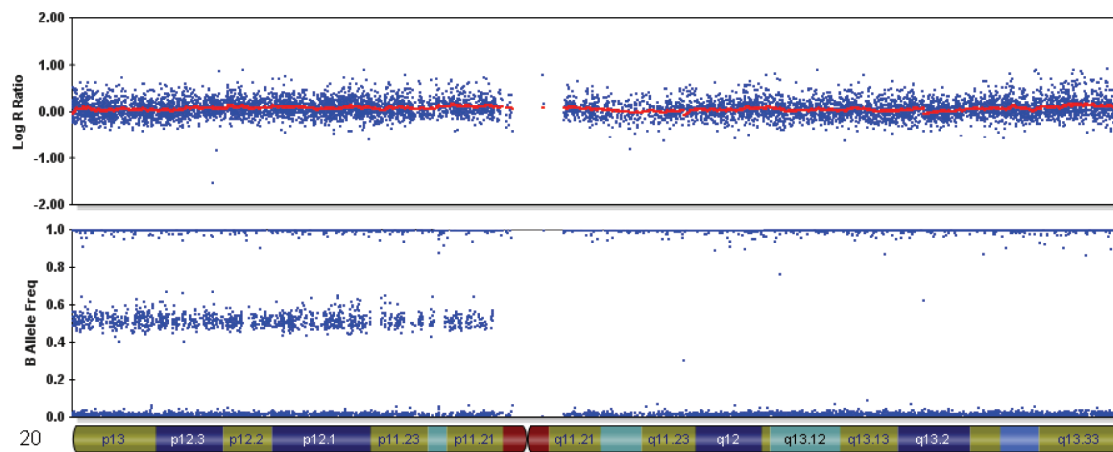


Figure 2.1 37.26 Mb region of LOH on chromosome 20q in case BC311 detected with the Illumina 317K BeadChip. Beadstudio logRatio estimate for each individual SNP in the first plot and genotype call for every SNP in the second plot. The X-axis shows the position on the chromosome.

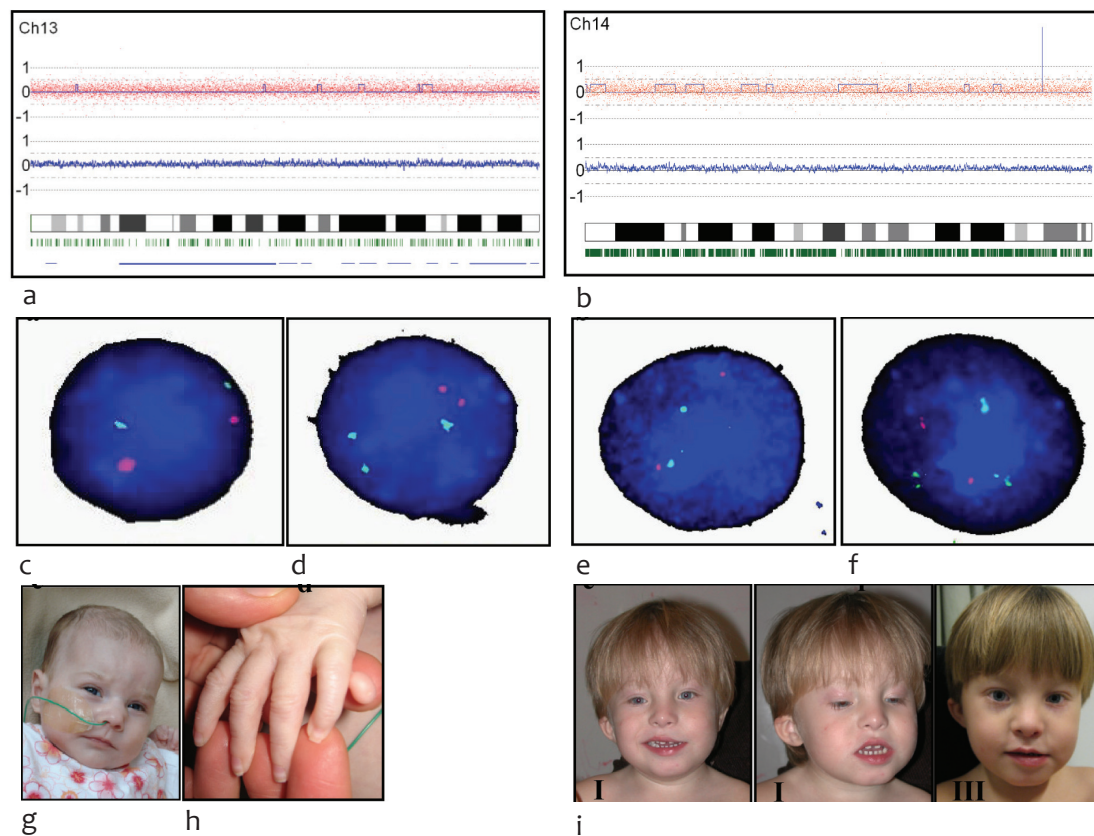


Figure 2.2 (a) CNAG copy number analysis for patient CR355 using the Affymetrix 262K GeneChip. LogRatio estimate for each individual SNP in the first plot and for an average of 10 SNPs in the second plot. Both plots show a slight increase in logRatio for whole chromosome 13. Blue line in first plot: copy-number estimate calculated with the Hidden Markov Model. The X-axis shows the position on the chromosome. Green stripes: heterozygous SNP calls. (b) CNAG copy number analysis output for patient CR377 using the Affymetrix 262K GeneChip. Both plots show a slight increase in logRatio for chromosome 14. (c) FISH experiment (probes LSI13 (green) and LSI21 (red), Vysis) showing a normal cell. (d) FISH experiment showing the presence of a mosaic trisomy 13 in 18% of the 200 cells analyzed. (e) FISH experiment (probes LSI CCNDI, 11q13 (red) and LSI IGH, 14q32 (green), Vysis) showing a normal cell. (f) FISH experiment showing the presence of a mosaic trisomy 14 in 9% of the 200 cells analyzed. (g) Facial picture of patient CR355. Facial dysmorphisms included upslant of palpebral fissures, a broad nasal bridge and uplifted earlobes. (h) Picture of postaxial polydactyly of the left hand of CR355. (i) Facial pictures of case CR377, 3 years and 7 months (I, II), and 4 years and 8 months (III). Note marked asymmetry when smiling, asymmetric upslanted palpebral fissures, left sided epicanthus, hypertelorism, low-set and small right ear.

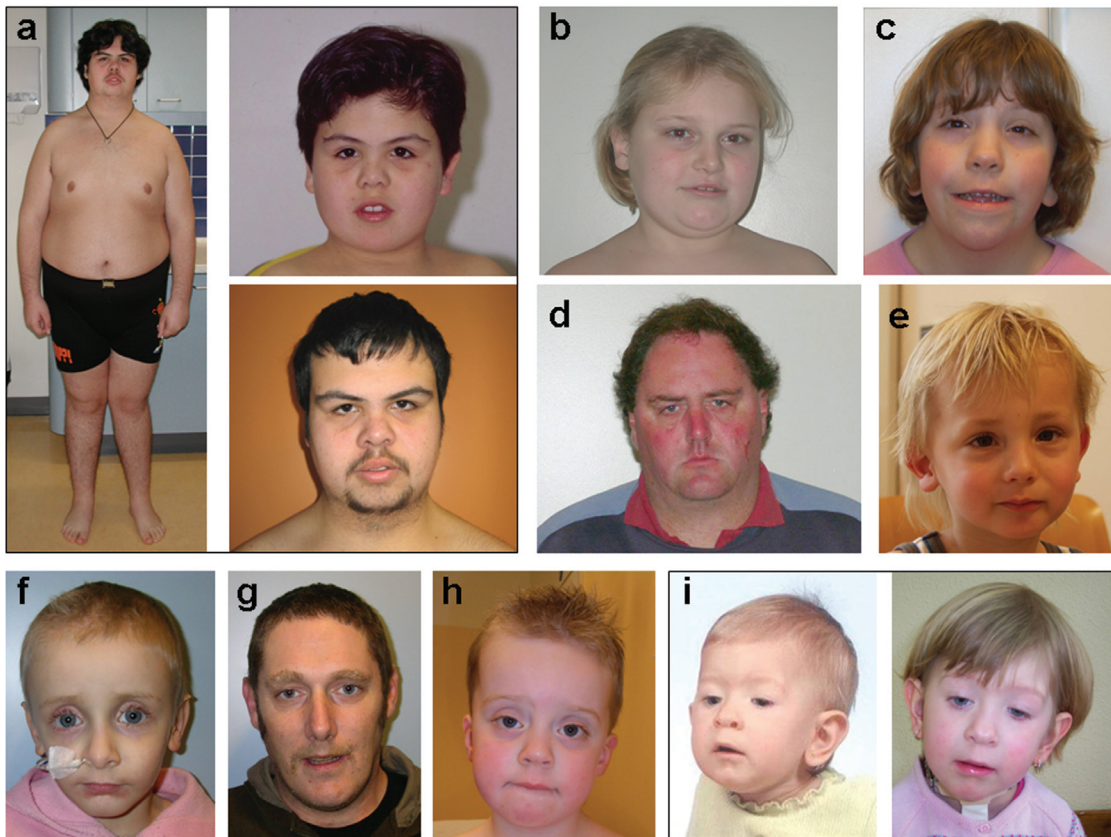


Figure 3.1.1 Phenotypical characteristics of cases with a 16p11.2 deletion. (a) case 2 (overview aged 16 years (left), face aged 7 years (top) and 17 years, (b) case 3, (c) case 6, (d) case 10, (e) case 11, (f) case 12, (g) father of case 12, (h) case 13, (i) case 14 (at the age of 9 months (left) and 4 years). Some of the cases share facial characteristics (long nose in cases 6, 12 and, father of case 12) (c, f, g); narrow palpebral fissures in cases 6 and 14(c, i); periorbital fullness in cases 2, 3, and 11(a, b, e); ptosis in cases 13 and 14 (h, i). Overall however, patients show no common facial features.

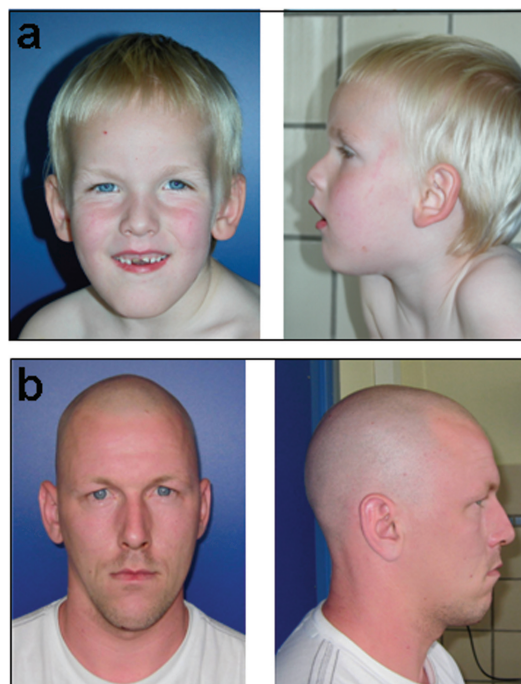


Figure 3.1.2 Facial characteristics of cases with an atypical 16p11.2 deletion. (a) case 15, (b) father of case 15. Note long narrow face, prominent forehead, downslanted and narrow palpebral fissures, and downturned corners of the mouth in both.



Figure 3.3.1 Patient 1 and his brother. (a) Patient 1 with elongated face and flat midface. (b) Scoliosis of patient 1. (c) Flat, thin and long feet of patient 1. (d) Brother of patient 1 with similar facial appearance. (e) Scoliosis and pectus excavatum of the brother. (f) Flat, thin and long feet with long first digits of the brother. (g) SNP array (Affymetrix Genome-Wide Human SNP Array 6.0) results of patient 1 showing a 12.5 Mb duplication. Log₂ratios for each probe are plotted against the position on the X-chromosome. Intensity values are compared with normal males and females resulting in Log₂ratios below zero for one copy of the X-chromosome for males. Duplicated regions have a Log₂ratio of 0, including the pseudoautosomal regions 1 and 2 (PAR 1 and 2) at Xp22.3 and Xq28.

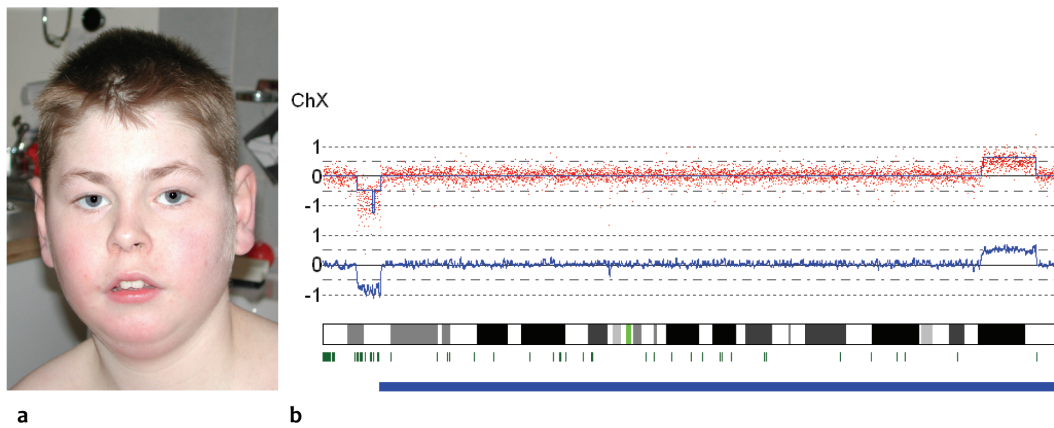


Figure 3.3.2 Patient 3. (a) Facial appearance showing oval eyes, short nose and a relative small chin. (b) SNP array (Affymetrix GeneChip Human Mapping 262K Nspl and 238K Styl) results showing the 2.71 Mb deletion and 6.22 Mb duplication. Intensity values are compared with normal males resulting in Log₂ratios of zero for one copy of the X-chromosome. Log₂ratios for each probe are plotted against the position on the X-chromosome.

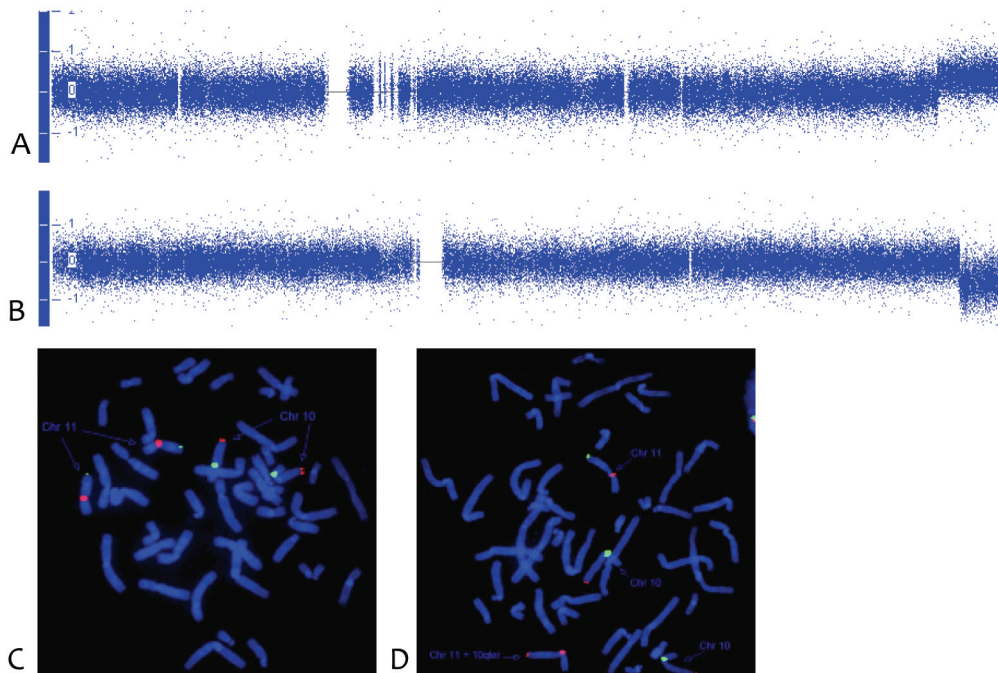


Figure 3.4.2 Case 1. (a) SNP array analysis revealed a duplication of 10.11 Mb on chromosome 10 and (b) a 7.51 Mb deletion on chromosome 11. (c) FISH analysis results showing a normal cell line and (d) a cell line with the $\text{der}(11)\text{t}(10;11)(\text{q}26.13;\text{q}24.2)$.

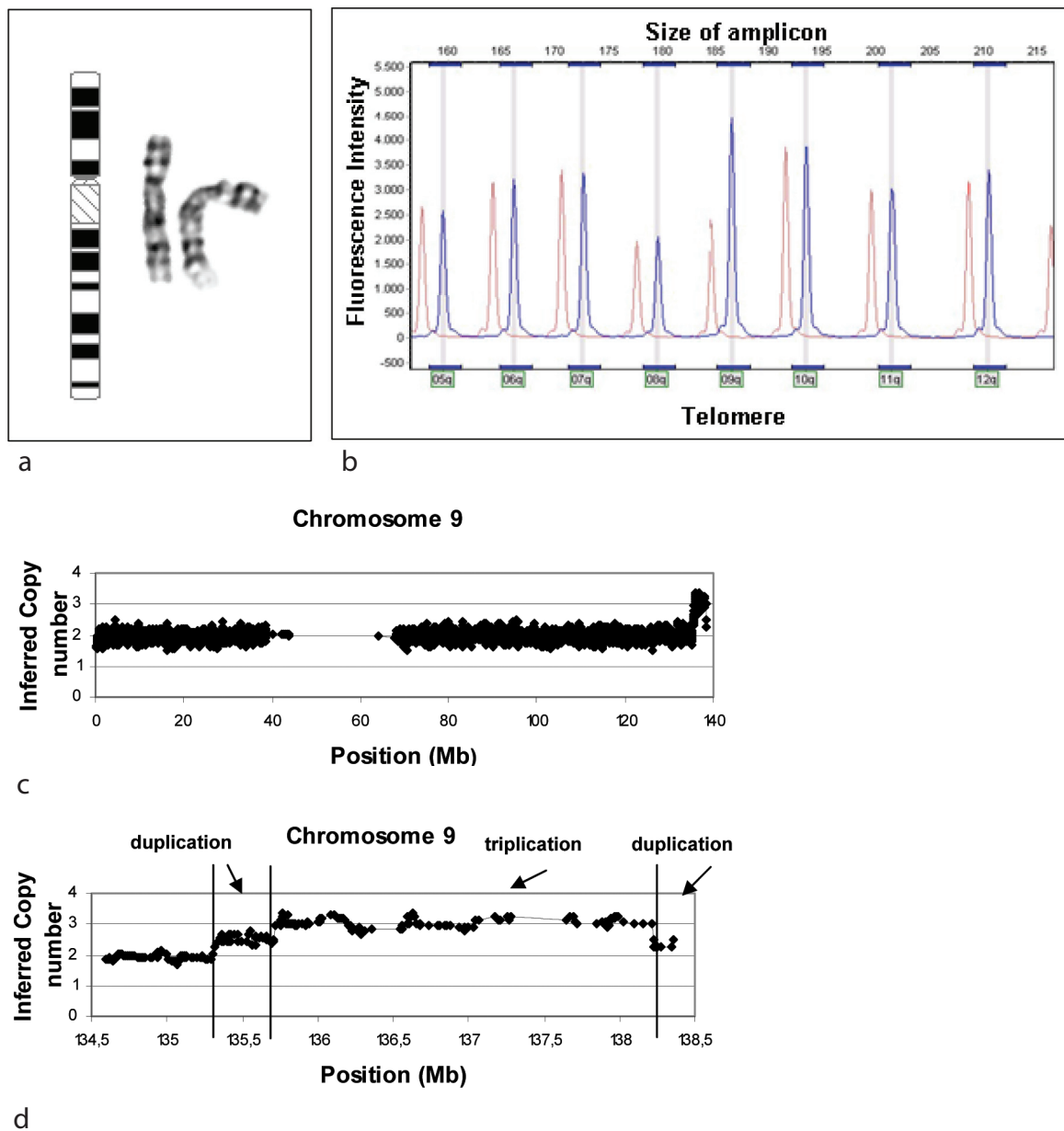


Figure 4.1.1 Cytogenetic and molecular results. (a) Partial karyotype showing both chromosomes 9. Right: abnormal chromosome 9. (b) MLPA analysis revealing an aberration of the 9q probe. Red peaks: control panel; blue peaks: patient. (c) SNP array analysis of the patient revealed an aberration on the long arm of chromosome 9 of approximately 2.93 Mb. The threshold for deletions and duplications is, respectively, 1.6 and 2.4. (d) SNP array copy number plot focused on the duplicated region of chromosome 9, showing a ~400 kb duplication, a ~2.4 Mb triplication and a ~130 kb duplication.

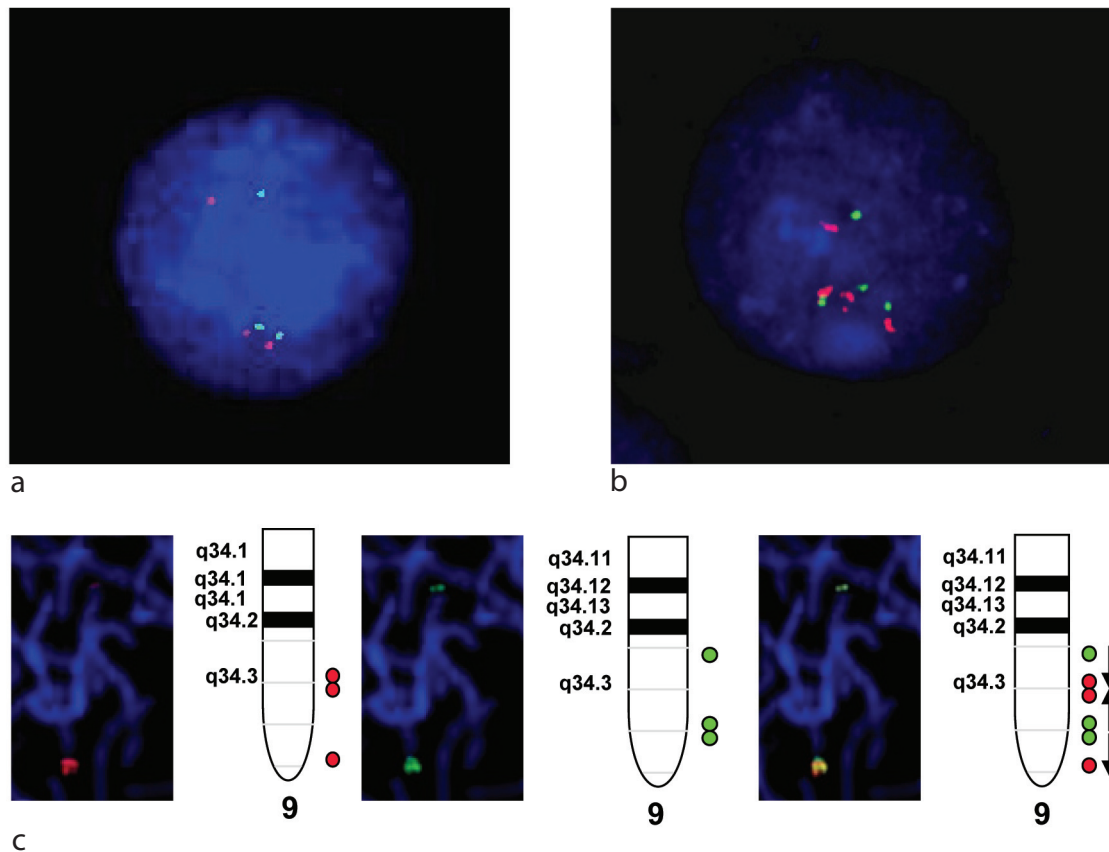


Figure 4.1.2 (a) FISH analysis with RP11-270D17 (green) and GS-135I17 (red) observed a duplication for both the probes confirming the 400 kb and 130 kb duplication, respectively. (b) Hybridization with RP11-413M3 (green, centromeric side of chromosome 9q) and RP11-48E05 (red, telomeric side of chromosome 9q) revealed the presence of four red and four green signals. The signals for the chromosome with the triplicated region showed that the middle repeat is inverted (green-red-red-green-green-red). (c) For probe RP11-48E05 the centromeric signal was of double intensity as compared to the telomeric signal. For probe RP11-413M3 (green) the telomeric signal was stronger than the centromeric signal. This indicates that the repeats of the triplication are normal in the proximal and distal region and inverted in the central region.

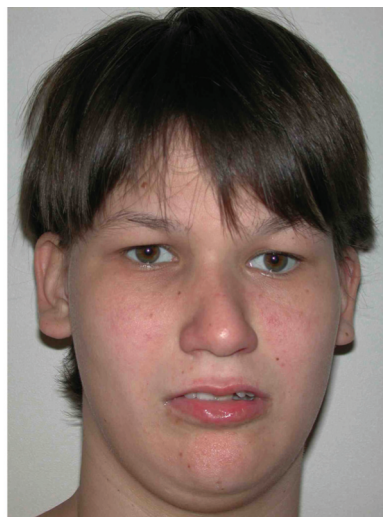


Figure 4.1.3 Picture of the female patient at the age of 16 years. Note mild facial asymmetry and narrow palpebral fissures.



Figure 4.2.1 Pictures of the index patient and her apparently healthy brother. (a) (b) Facial picture of the index patient at the age of 3 (a) and 4 (b) years. Note frontal bossing, hypotelorism and thin and long face. (c) Facial picture of her brother at the age of 2 years.

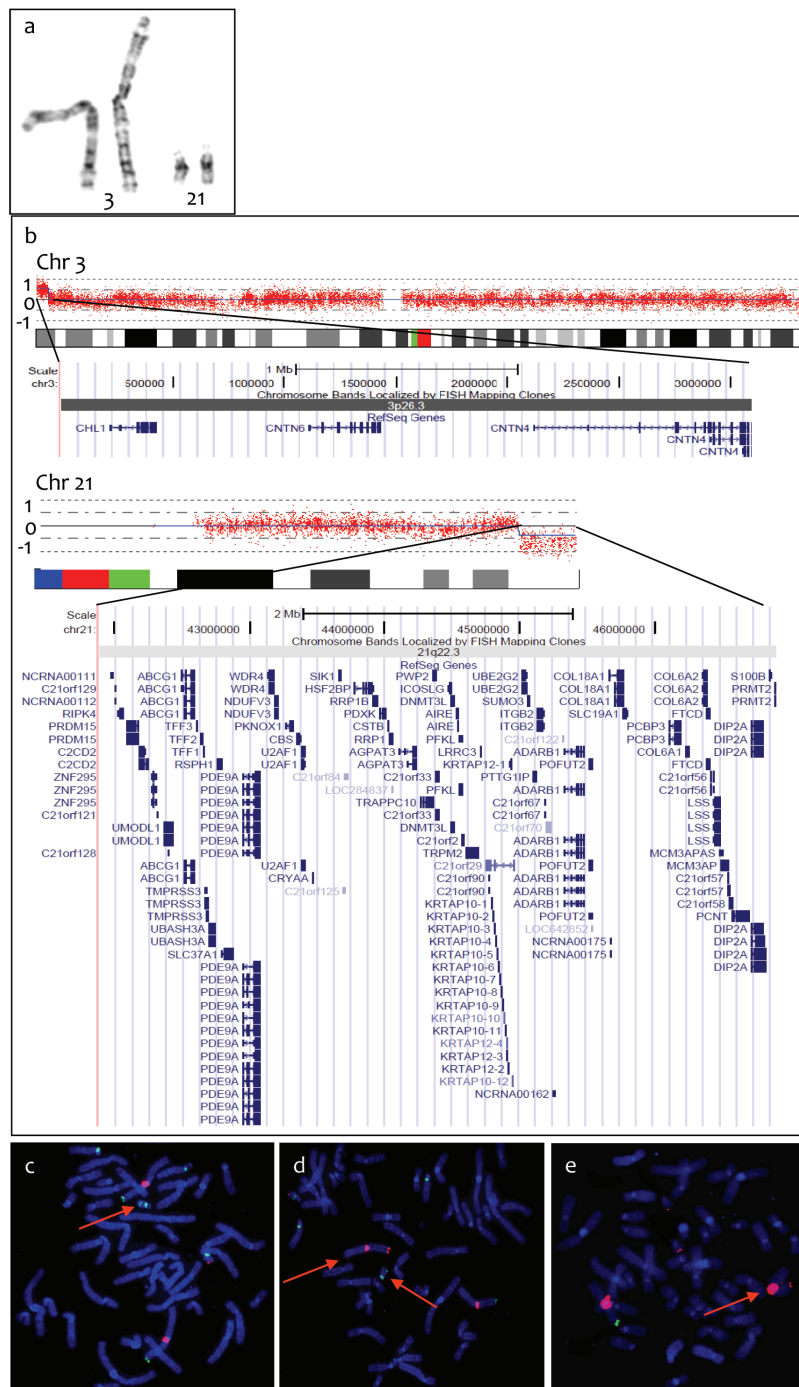
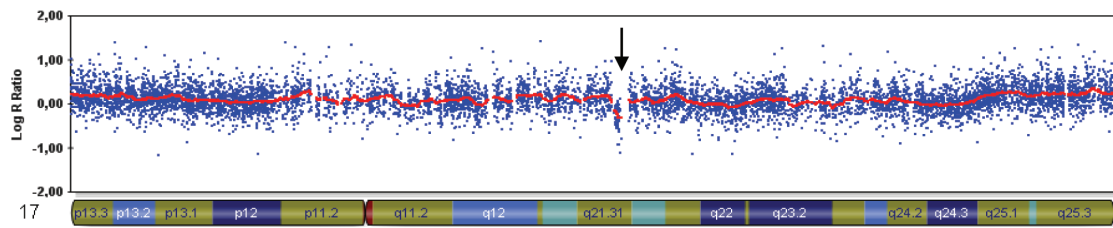
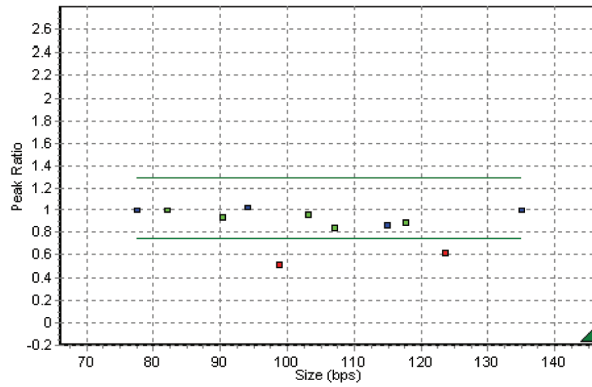


Figure 4.2.2 Cytogenetic and molecular analysis of the familial $t(3;21)(p26.3;q22.3)$. (a) Conventional karyotyping revealed no abnormalities for chromosomes 3 and 21 in the index patient. The arrow indicates the aberrant chromosome 21. (b) SNP array analysis (Affymetrix GeneChip Human Mapping 262K Nspl) results for the index patient demonstrating a 3 Mb duplication on the short arm of chromosome 3 and a 5 Mb deletion on the long arm of chromosome 21. Genes involved on both regions, UCSC Human Genome Browser (<http://genome.ucsc.edu>), Mar 2006 build (hg18). (c) FISH analysis confirmed the presence of the derivative chromosome 21 (black arrow), originating from a translocation between 3p (green; GS-1186B18; Flint) and 21q (red; GS-63H24; Flint). Control probes used for centromere chromosome 3 (red; CEP3; Vysis) and satellites of chromosome 13 and 21 (green; a-sat 13/21; Cytocell). (d) FISH analysis for the mother of the index patient demonstrated that she is carrier of the balanced $t(3;21)(p26.3;q22.3)$ (black arrows) (probes: GS-1186B18, GS-63H24, CEP3 and a-sat 13/21). (e) FISH analysis for the brother of the index patient showing the derivative chromosome 3 (black arrow) (probes: GS-1186B18, GS-63H24, CEP3).



a



b



c

Figure 5.1.1 Case 2 (a) Deletion of chromosome 17q21.31 (485 kb) found with the Illumina's Sentrix HumanHap300 Genotyping Beadchip. (b) MLPA analysis confirmed the deletion. Deleted probes: MAPT and KIAA1267. (c) Picture of the eyes of case 2, characterized by blepharophimosis, bilateral upper lid ptosis, epicanthus inversus and telecanthus.

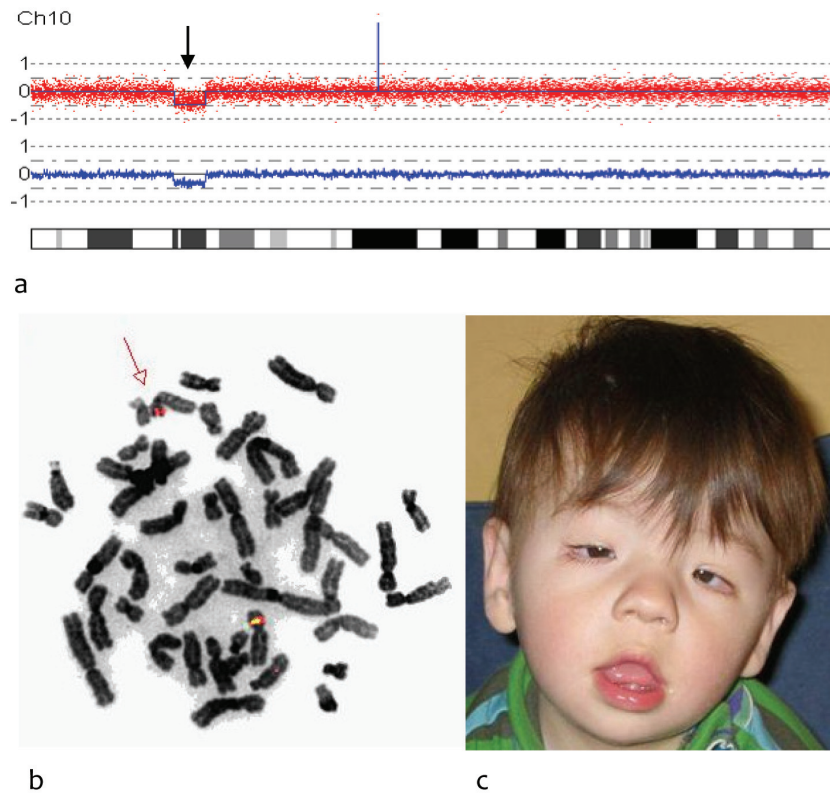


Figure 5.1.2 Case 4 (a) Deletion of chromosome 10p12.33-p12.31 (4.5 Mb) detected with Affymetrix GeneChip Human Mapping 262K Nspl. (b) FISH analysis confirmed the deletion. Control probe: RP11-390B4 (red), deleted probe 10p12.31: RP11-177H22 (green). (c) Facial picture of case 4, showing blepharophimosis, ptosis, epicanthal folds, ectropion of the lower eyelid, S-shaped upper eyelid, synophrys.

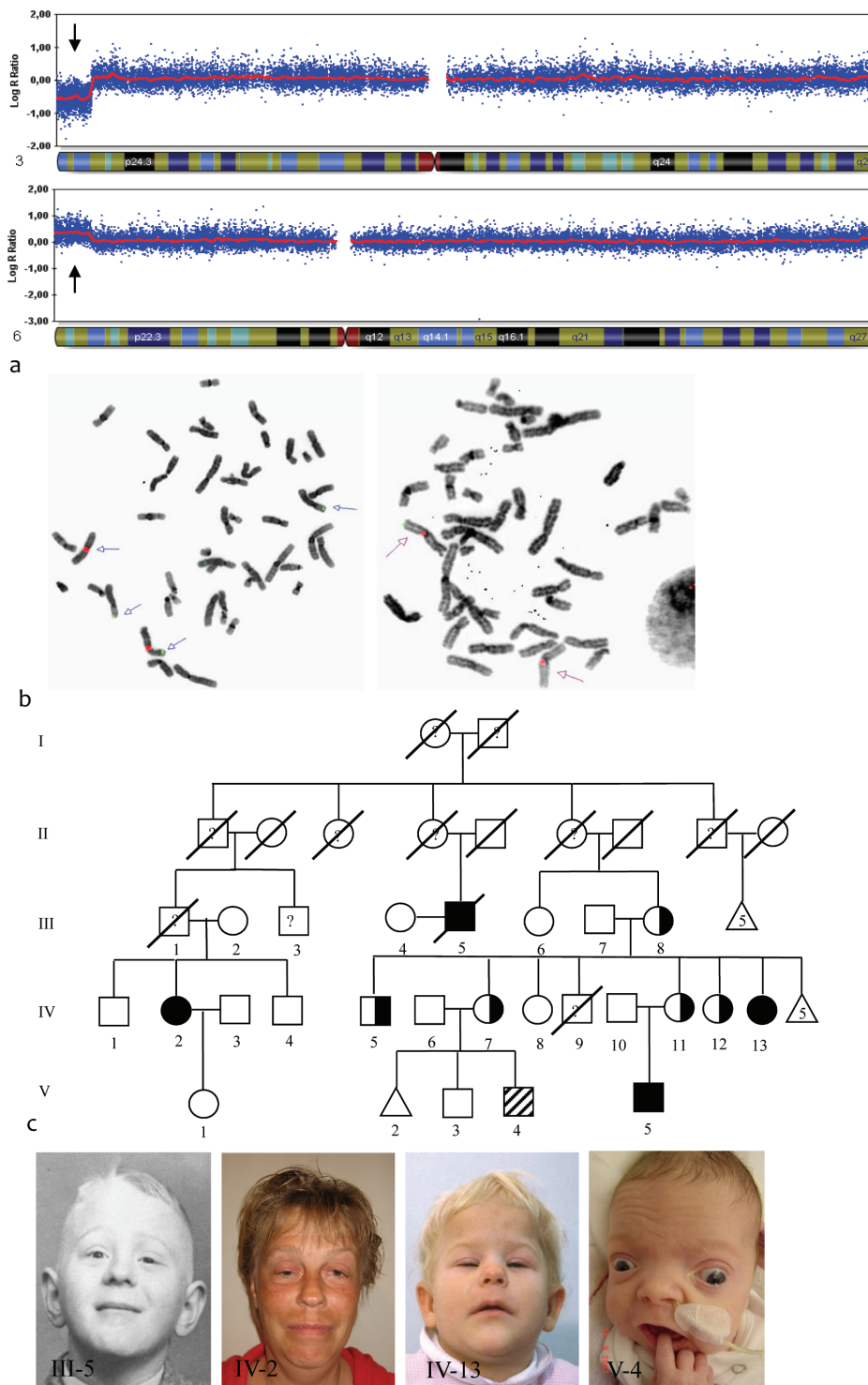


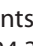


Figure 5.1.3 Case 9 (a) Terminal deletion of chromosome 3p25.3 (8.6 Mb) and terminal duplication of 6p24.3 (7.7 Mb) detected with the Illumina's Sentrix HumanHap300 Genotyping Beadchip. The derivative chromosome 3 was not observed by conventional G-banding. (b) FISH analysis revealed the presence of an unbalanced 3;6 translocation. Left panel, control probe: CEP3 (red) (Vysis), 6pter probe: GS-19615 (green); right panel, control probe: CEP3 (red) (Vysis), 3pter probe; GS-186B18 (green). (c) Pedigree of the family with the segregating t(3;6) analyzed with FISH experiments.  : balanced t(3;6);  : 3p25.3 deletion and 6p24.3 duplication;  : 3p25.3 duplication and 6p24.3 deletion. (d) Facial picture of case 9 (IV-2), characterized by blepharophimosis, ptosis, flattened and broad nose. Facial pictures of two relatives (III-5, IV-13) with the same unbalanced translocation as case 9 are presented. These members show similar clinical features. In addition, a facial picture of a relative (V-2) with the opposite unbalanced translocation is shown. No BPES-like features are seen in this child.